Rheol Acta (2002) 41: 514–523
DOI 10.1007/s00397-002-0249-8

ORIGINAL CONTRIBUTION

Claude Verdier
Matthieu Brizard

Understanding droplet coalescence and its use to estimate interfacial tension

Received: 10 January 2002
Accepted: 2 April 2002
Published online: 26 June 2002
© Springer-Verlag 2002

C. Verdier (✉) · M. Brizard
Laboratoire de Rhéologie,
Université Joseph-Fourier,
Institut National Polytechnique, CNRS
(UMR 5520), BP 53 – Domaine
Universitaire, 38041 Grenoble cedex 9,
France
E-mail: Verdier@ujf-grenoble.fr

Abstract The study of coalescence of polymer droplets is presented in the viscosity ratio range (p) going from 0.1 to 10. It is shown that the determination of the characteristic time of coalescence is a good way to estimate the interfacial tension. Polydimethylsiloxane (PDMS) is mixed with polyisobutylene (PIB) and the temperature change provides a way to modify the interfacial tension of the PDMS/PIB system significantly, as measured using a pendant drop apparatus. We obtain a dependence of the reduced coalescence time as a function of $p^{-1/2}$ which gives access to the interfacial tension. This technique can be an interesting choice for estimating interfacial tension without requiring sophisticated techniques.

In a further attempt to correlate these observations with a theoretical model (Verdier C (2001) Polymer 42), the flow field inside and outside the droplets is investigated. PIV measurements are carried out where the evidence of elongational regimes is demonstrated. Such experiments are also interesting for future comparisons with numerical results.

Keywords Coalescence · Polymer · Elongation · Viscosity ratio · PIV

Introduction

Understanding the mixing of two polymers requires to know about the rheological properties of the fluids, to be able to determine flow fields, but also to control the interfacial properties of such fluids. As a start one may study the droplet breakup and coalescence of Newtonian fluids, since these two mechanisms govern the final properties of the mixture (Fortelny and Zivny 1995a). Taylor has studied breakup (Taylor 1934) in his seminal paper and he found a criterion for breakup depending on the viscosity ratio of the fluids. Let us denote by p the viscosity ratio η_1/η_2, η_1 being the viscosity of the droplets (suspended fluid) and η_2 the viscosity of the suspending fluid. The capillary number can be defined by $C_a = \frac{\eta_2 \dot{\gamma} R}{\sigma}$, where σ is the interfacial tension, R is the radius of the droplet and $\dot{\gamma}$ is the shear rate. At small deformations, the product of the capillary number by the function $f(p) = (19p + 16)/(16p + 16)$ equals the deformation (Taylor 1934). On the other hand, when the droplet undergoes high deformations, for example at high shear rates, the droplet becomes elongated and eventually breaks into two parts or more: the greater the shear the more droplets. Grace (1982) plotted experimentally the variation of the critical capillary number Ca_c above which the spherical droplet breaks, as a function of p, over ten decades, both in shear and elongational flows. In such flows, the shear rate $\dot{\gamma}$ should be replaced with $2\dot{\varepsilon}$ (elongational rate $\dot{\varepsilon}$). Grace (1982) noticed that no breakup occurs in shear flows when p is larger that 3.5 approximately, and that it is easier to break spherical droplets in elongation than in shear. Modeling such results is possible when small deformations are involved. Barthès-Biesel and Acrivos (1973) calculated the onset of bursting of small droplets in a shear flow using a perturbation theory around the creeping-flow solution and found good agreement with experiments. Later, experiments by Bentley and Leal

(1986) combined with the numerical simulations of Stone and Leal (1989) allowed one to determine the range of validity of the available models, as well as the influence of the initial shape or degree of deformation of the droplets. Two interesting reviews are also available on this subject (Rallison 1984; Stone 1994).

Finally, in a two-phase flow, when the shear rate is varied, one may find a dependence of the final radius of the droplets as the inverse of the shear rate, since the critical condition occurs at a fixed capillary number.

Regarding the coalescence phenomenon, which is directly in competition with break-up during mixing, much less is known. Janssen and Meijer (1995) provide a similar criterion for the final droplet size during shearing and give a relationship between the radius of the resulting droplets and the shear rate. A power dependence –0.6 is obtained. Comparing these behaviors in a shear flow (Grizzuti and Bifulco 1997; Vinckier et al. 1998) is then possible and can give information about which type of mechanisms (coalescence or break up or both) takes place when mixing two fluids.

Coalescence can also be regarded as an interesting mechanism, driven by interfacial tension, which can exist even when no shear is applied. Droplets can coalesce simply by interacting with each other. Usually, with polymers, van der Waals interactions are sufficient for droplets to merge into a larger resulting droplet. Chesters (1991) studied this phenomenon in detail, in particular the approach between the droplets which gives rise to drainage of the interstitial fluid (fluid 2) until the droplets coalesce. Liquid droplet coalescence has been studied by Eggers and coworkers (Eggers et al. 1999, see also references therein), who paid good attention to the first instance of the process. Martula et al. (2000) also studied the effect of coalescence on coalescence itself, i.e., in a concentrated droplet system. The case of polymers and compatibilizers has also received much attention (Fortelny and Zivny 1995b; Sundararaj and Macosko 1995). Recently, Verdier (2000, 2001) paid attention to the flow involved by the coalescing droplets, after they come into contact, and studied the shape of the resulting droplet experimentally to determine the dependence of the coalescence time as a function of the viscosity ratio p. Three regimes were found, each one with a typical slope as a function of p. The most interesting is that obtained when the fluids have comparable viscosities ($0.1 < p < 10$), because such situations are commonly met in mixing devices. In this case, the coalescence time varies like the geometric mean of the viscosities (Verdier 2000).

This method is investigated further in this paper, one of its aims being to find a relationship between the coalescence time and the viscosity ratio, in order to come up with another way to estimate the interfacial tension. This part is presented next, using two polymers (PDMS and PIB). Changing the temperature is a way to monitor the interfacial tension as well as viscosities. It is shown that the knowledge of the viscosities of the fluids and the coalescence time are sufficient to have access to the interfacial tension. The influence of the radius ratio between the droplets is also taken into account. The results are presented in the first section. In the second part of the experimental section, PIV measurements will also be shown: these measurements are indeed very important to investigate the flow field further, and may also be useful to compare with computations. It is shown that elongational flows are dominant close to the center of the resulting droplet during coalescence. This method should eventually be used further to calculate the viscous dissipation exactly during coalescence. It may be useful to determine the exact dependence of the coalescence time on p theoretically.

Materials and experiments

Fluids and properties The two fluids which were selected are polydimethylsiloxane (PDMS, 47VT60000, Rhône-Poulenc, $M_w = 116{,}500$ g/mole, $M_n = 62{,}400$ g/mole) and polyisobutylene (PIB, Parapol 950, BP Chimie, $M_w = 1472$ g/mole, $M_n = 932$ g/mole). These types of fluids have been used previously (Grizzuti and Bifulco 1997; Verdier 2000, 2001) and provide adequate properties for visualization. Indeed their refractive indexes are close and allow visualization of one fluid inside the other and vice versa. Their rheological properties are known accurately and they are shown to behave like Newtonian fluids when the velocity gradient is small (typically $\dot{\gamma} < 1000 s^{-1}$ at 20 °C), which will be the case since times involved in the coalescence experiments are rather long (of the order of seconds). Experiments will be carried out at different temperatures ranging from 20 °C to 60 °C, allowing for a viscosity ratio change, as well as changes in the interfacial tension. The viscosities are indeed required for the investigation of the coalescence time. Figure 1 shows this dependence of the viscosity as a function of temperature.

Since large changes are obtained, a semi-log scale was used which shows a typical linear dependence of the log(viscosity) as a function of temperature. As expected for PDMS, the viscosity change is not so large, going from 66 Pa.s to 30 Pa.s in the range 20–60 °C. On the other hand, the PIB viscosity shows larger changes in the same range, going from 62 Pa.s (at 20 °C) to 2 Pa.s (60 °C) roughly. This interesting behavior allows one to cover a viscosity ratio p going from about 1 to 15, when PDMS is the dispersed phase. On the other hand, when PDMS is the matrix, we cover the symmetric range from 0.067 to 1. This allows us to recover the interesting range where the viscosity ratio p goes from about 0.1 to 10. This will provide another verification of the previous results, by changing temperature rather than changing fluids.

The interfacial tension between PDMS and PIB was obtained on a usual pendant drop apparatus (Digidrop), using PDMS inside PIB, with a temperature ranging between 20 and 60 °C. Density measurements are required and were taken from previous experiments (Longin 1999). The results for interfacial tension are presented in Fig. 2.

An approximately linear dependence is obtained as in the literature for usual polymer pairs (Wu 1982). Data concerning the temperature dependence for this PDMS/PIB system has been published in the literature (Wagner and Wolf 1993), and is in the range between 2.5 and 4 mJ/m^2 for PDMS/PIB systems, but it is strongly influenced by the molecular weight. It may also be a nonlinear function of temperature, as it passes through a maximum

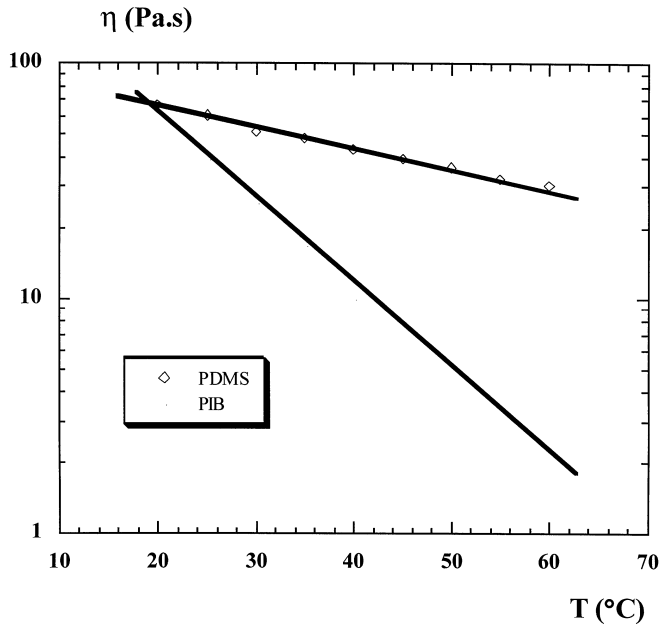

Fig. 1. Polymer viscosities (PDMS and PIB) vs temperature

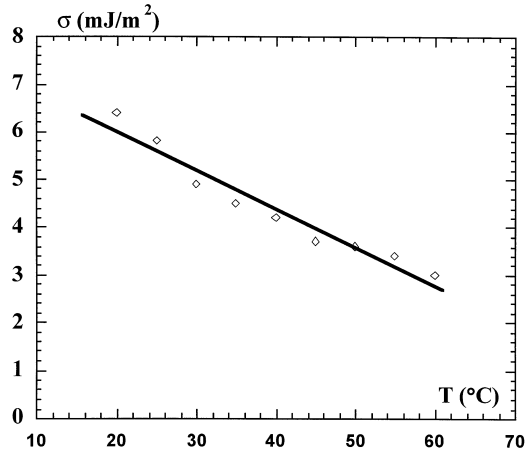

Fig. 2. Interfacial tension for PIB/PDMS system as a function of temperature

for some systems. On the other hand, it is close to 3 mJ/m^2 at room temperature for similar systems (Grizzuti and Bifulco 1997). Our values are found to be slightly higher but in reasonable agreement to the first data in the same temperature range. This may be due to manufacturing, i.e., the molecular weights and molecular weight distribution may differ from similar fluids used. Indeed the surface tension of each component usually increases with molecular weight.

Droplet coalescence This technique has been previously investigated and was improved recently (Verdier 2001) to study the effect of the viscosity ratio $p = \eta_1/\eta_2$, where 1 refers to the droplet and 2 corresponds to the suspending medium. Six decades in viscosity ratio were covered and the coalescence time was introduced. After bringing the two fluids together in a small container (a few mg of each), they are mixed with a spatula slowly until droplets are formed, showing a rather monodisperse emulsion. Typical droplet radii are between 5 and 20 μm, but sizes may be adjusted depending on the mixing time: the longer the mixing the smaller the size, because breakup is increased. Then the system is allowed to stand until droplets are spherical, and also to let air bubbles out if present. Putting the system between a glass plate and a micro coverglass allows proper visualization of the system (magnification ×20 or ×50 gives good quality pictures). There should be enough droplets but not too many, to avoid unwanted interactions between them. One can localize the droplets away from edges, so that end effects are avoided. Let D(t) be the length of the resulting axisymmetric droplet. A typical curve showing $D(t)/D_0$ is shown in Fig. 3, as well as a sketch of the droplets.

D_0 is the initial length of this so-called composite droplet and equals $2(R_1 + R_2)$, where R_1 and R_2 are the initial droplet radii just before the droplets coalesce. As in previous works, we introduce a typical coalescence time, as the inverse of the negative slope at the inflexion point (t_i) on the curve $D(t)/D_0$ vs time t; in other words

$$t_c = -D_0/D'(t_i) \quad (1)$$

This technique has been justified by the fact that the onset of coalescence ($t = 0$) is difficult to catch experimentally and therefore the method using the slope is more accurate. The evolution of the time dependence of the distance D(t) is followed using an optical microscope (Leica, DML model, magnification ×20 or ×50) using transmitted light, and recorded through the use of a camera (3-CCD color, KY-F55B JVC model, 25 frames/s) onto a video recorder (U-Matic, SP type, VO-9600P model). Due to the values of the refractive indexes, no particular treatments or methods are required for observation. D(t) shows first a rapid decrease, until it eventually levels off due to the final relaxation of the droplet. The final stage can also be used for measuring the interfacial tension (Luciani et al. 1997) using a previous theory (Rallison 1980). This latter technique is very valuable and works at small droplet deformation but it may be difficult to create an ellipsoid axisymmetric droplet. In our case, axisymmetric droplets have always been obtained due to the initial conditions, i.e., two spherical droplets.

Influence of the radius size In previous works, the same droplet sizes were used but this was a drawback of the technique. We present here another way to process the data, allowing for different droplet sizes. Since the coalescence time t_c (Fig. 3) is the slope at the inflexion point, t_c should be the time required for going roughly from $D_0 = 2(R_1 + R_2)$ to $D_\infty = 2R_e$, where $R_e = (R_1^3 + R_2^3)^{1/3}$ is the final radius of the resulting droplet, given by mass conservation. Therefore a typical relevant length scale R should be

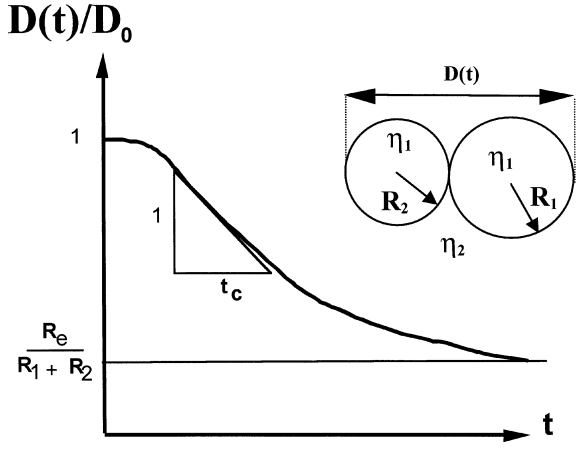

Fig. 3. Sketch of the $D(t)/D_0$ curve ($D_0 = 2R_1 + 2R_2$) and characteristic time t_c

$$R = (R_1 + R_2) - R_e \quad (2)$$

Then let us use the following dimensionless parameters. $p = \eta_1/\eta_2$ is the viscosity ratio and the reduced time of coalescence t_c will be defined as $\sigma t_c/\eta_1 R$. This definition is more general and allows one to account for different droplet sizes.

Coalescence time vs viscosity ratio Several experiments at temperatures 20, 25, 30, 35, 40, 45, 50, 55, and 60 °C were carried out to study droplet coalescence. Many droplet sizes were chosen. Droplets already close to each other were selected to minimize the time it takes for draining the outer fluid. The reduced time of coalescence obeys a law similar to the previous ones (Verdier 2000). This is described in Fig. 4, where $\sigma t_c/\eta_1 R$ is plotted as a function of the viscosity ratio η_1/η_2 over two decades.

The linear fit obtained shows a power law dependence of –0.5 and the reduction technique is valid at all temperatures. The constant is somewhat different from the previous one because of the new length R chosen in the dimensional analysis. We find

$$\sigma t_c/\eta_1 R = 118.2(\eta_1/\eta_2)^{-0.5} \quad (3)$$

All the data points seem to be aligned quite well and therefore it is possible to use this technique inversely to have an estimation of the interfacial tension. Indeed, once the viscosities are known it is possible to invert Eq. (3) to have access to σ. Still one may observe that this technique is only based on an order of magnitude analysis, not an exact formula.

The error on the measurement is rather small due to the fact that excellent accuracy is usually found both for times and radii measurements (through the microscope). This method is promising for investigating the interfacial tension of polymeric materials, and the advantage is that it does not require a sophisticated apparatus. Preparation is rendered easier because of the simple mixing procedure, which does not require one to insert droplets into another fluid using complicated devices.

The formula at Eq. (3) is rather hard to predict theoretically unless making assumptions. Nevertheless, using the idea that most of the flow close to the nip governs the viscous dissipations, one can assume lubrication in this region and show (Brochard-Wyart and de Gennes 1992, 2000) that the predicted reduced coalescence time varies like $p^{-2/3}$ (Verdier 2001). Unfortunately, this is not exactly the case here. Therefore, a more precise model requires the exact determination of the flow field, which is carried out next.

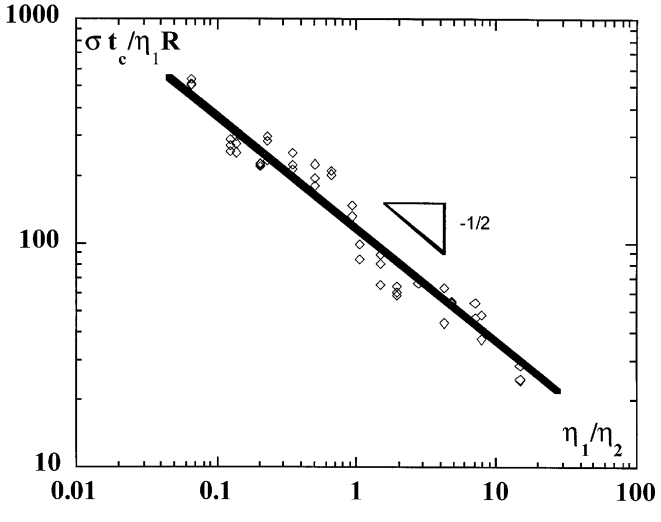

Fig. 4. Dimensionless coalescence time vs viscosity ratio $p = \eta_1/\eta_2$ (PDMS/PIB system at different temperatures)

PIV measurements

Fluid preparation and methodology

Droplets were filled with small particles ($CaCO_3$, size about 1 μm or smaller). Careful preparations were carried out in order to have a homogeneous distribution of particles. We have limited our interest to the region inside the droplets, otherwise pictures would look too difficult to understand. Sometimes it is possible that a few particles may appear outside droplets, but in a non-significant manner. A limited number of particles is used so that no aggregation is possible. Also we want to make sure that the viscosities of the fluids do not change significantly. In order to achieve this mixing, particles are first isolated on a glass piece and spread out with a spatula so that they cannot aggregate. They are put in the oven and allowed to dry. After 2 h fluid 1 is mixed gently with the particles until a homogeneous mixture is obtained. Verification is done under the microscope. If it is satisfactory, then fluid 2 (i.e., the matrix) is added to fluid 1, as in the case of the coalescence experiment described before. Again the system is put between the glass plate and micro cover-glass and is ready for observation. The same procedure is used to achieve coalescence. Then films are used as an input to the PIV processing system (Dantec). Pictures are separated by 0.04 s at best and may be used for determining flow fields and streamlines. In order to have a good resolution it is sometimes better to use more distant pictures (timewise) to obtain a sufficient particle displacement.

Qualitative results

An example of the flow field is shown in Fig. 5a–f. The size of the droplets can be seen from the microscope scale. In addition, a second scale (arrow) has been added for the velocity magnitude. This is a non-stationary problem and streamlines need to be computed at each time step. In the series of pictures the system was PDMS inside PIB at a temperature of 50 °C.

Let us first point out that this case corresponds to droplets of equal sizes. Different droplet sizes will be discussed later. In this case, the flow field is axially symmetric with respect to the (Oz) axis, in cylindrical coordinates.

- Figure 5a is taken at time t = 0.24 s, very close to the start. One can see the very rapid motion of the neck, with velocities close to 4 μm/s already. The neck is showing a large curvature, as already mentioned in previous works (Frenkel 1945; Kuczynski 1949; Mazur and Plazek 1994). Note also that motion within the droplets is starting slowly and that velocities are much smaller far from the neck.

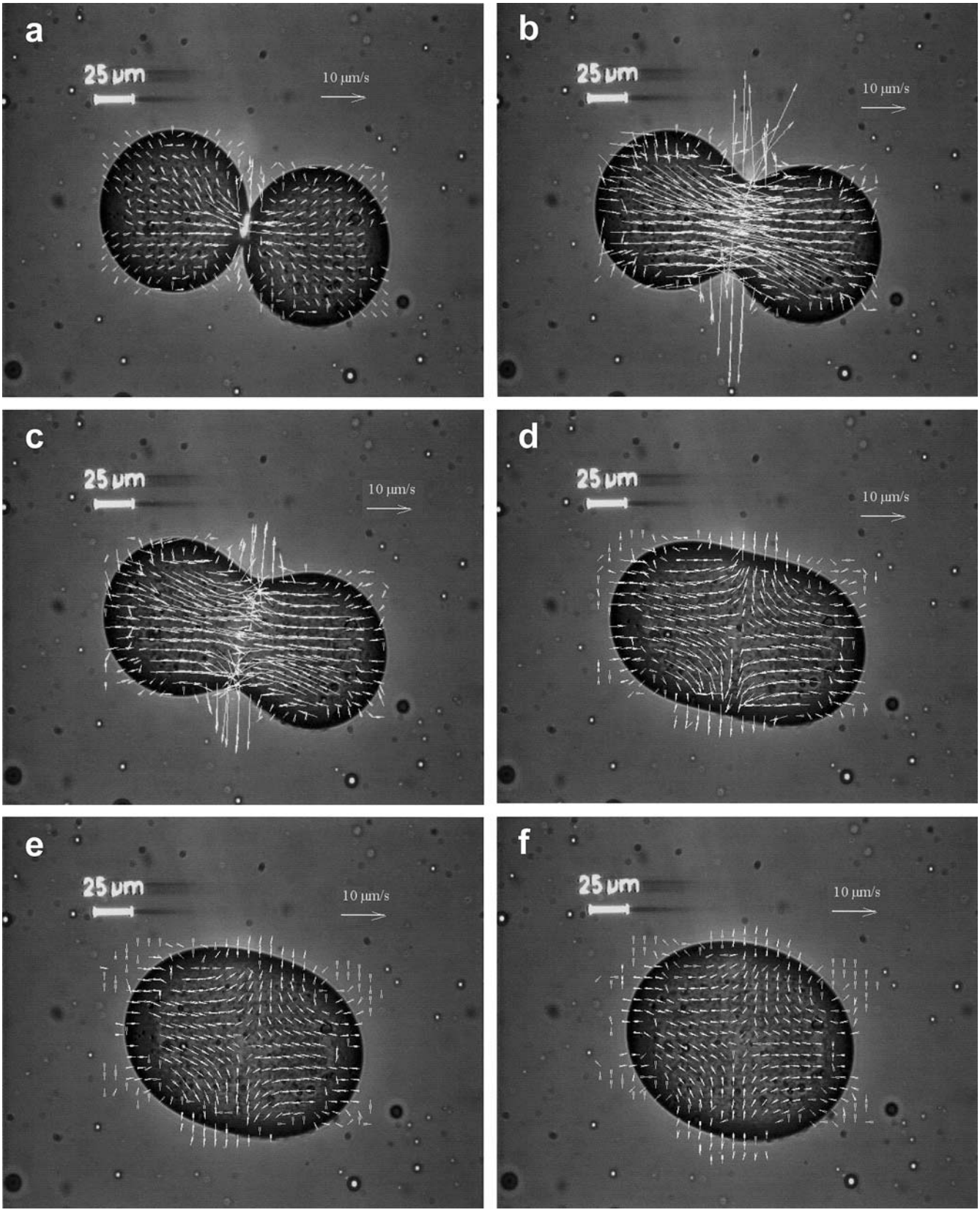
a
25 µm
10 µm/s
b
25 µm
10 µm/s
c
25 µm
10 µm/s
d
25 µm
10 µm/s
e
25 µm
10 µm/s
f
25 µm
10 µm/s

◄

Fig. 5a–f. Flow field at time: (PDMS inside PIB, T = 50 °C), $\eta_1 = 36$ Pa.s, $\eta_2 = 5$ Pa.s, $R_1 = 49$ μm, $R_2 = 49$ μm; **a** t = 0.24 s; **b** t = 1 s; **c** t = 1.48 s; **d** t = 4 s; **e** t = 6 s; **f** t = 8 s

- At a later time of t = 1 s (Fig. 5b) the flow within the droplets has become more significant: the two droplets are merging. Velocities at the neck ring are very important, in the range of 20 μm/s, probably close to their maximum value.
- The next picture is taken at t = 1.48 s (Fig. 5c). The velocity at the neck is now decreasing slowly after having reached a maximum. The flow field near the center of the droplets looks like a uniaxial elongational flow, with a time-dependent stretching rate.
- Figure 5d (t = 4 s) shows the resulting droplet at the point where the neck just disappears. Again the flow is clearly of elongation type close to the center. Velocities are still decreasing.
- At t = 5 s (Fig. 5e), relaxation is starting. This experiment is comparable to the ones described previously (Luciani et al. 1997; Guido and Greco 2001) and the droplet slowly starts to round like a sphere. Velocities are small everywhere (around 1 μm/s).
- Time t = 8 s shows an almost spherical droplet (Fig. 5f). The coalescence process is almost complete. Velocities are hardly measurable and are close to 0.

This gives an idea of the flow field inside droplets, but it is also of interest to show a complete picture of the flow field, inside and outside droplets. The overall flow field is needed in order to determine dissipations.

Figure 6 shows the overall velocity field. We have used particles inside the droplets and outside. Few are necessary otherwise the picture would become hard to read. Let us note the presence of the elongational flow region at the droplet center, as discussed above, although it is not a uniaxial one, due to different droplet sizes. One can pay attention to the presence of recirculating flows outside the droplets, due to the fact that fluid 2 is displaced outwards at the neck, and on the other hand it is slowed down later in the surrounding fluid at rest. Fluid 2 comes back towards the droplet due to the interface motion which pulls it again towards the droplet center. This creates a recirculating motion at each given time (t = 1.24 s here). This is different from other works (Eggers et al. 1999; Martula et al. 2000) where the authors simply sketch the flow field without noticing that recirculations are needed to create drop shape relaxation. Figure 6 seems quite realistic and may be useful to predict coalescence-induced coalescence (Martula et al. 2000).

Velocity data

The PIV technique presented is therefore a very good tool for monitoring the flow field within droplets. Also measurements at special points of interest can be made easily. Such points are the end points, the points on the neck ring, and the region at the center of symmetry which is also of interest. Data at such points is shown next.

At typical points defined in Fig. 7, the velocity vector is along the r-axis (A and B, points on the neck ring) and along the z-axis (C and D, end points). The evolution of the velocities of these points, namely V_A, V_B, V_C, V_D, is shown in Fig. 8, as well as the distance D(t) and the evolution of the distance corresponding to the neck r(t), defined in Fig. 7. These velocities have been measured

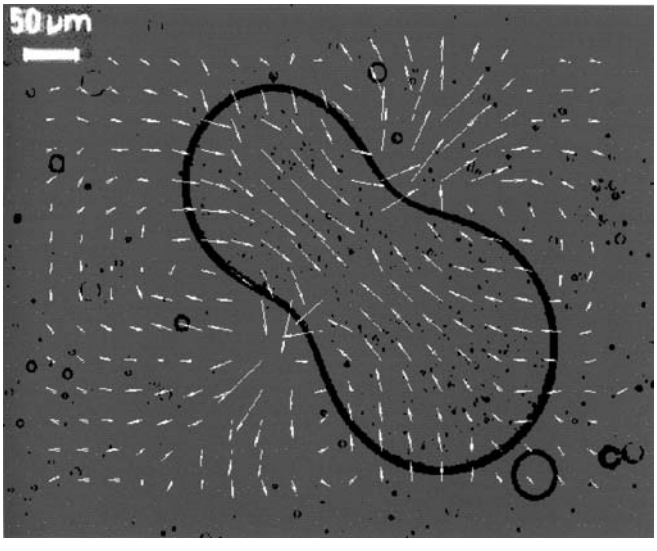

Fig. 6. Complete velocity field (inside droplets and outside) at t = 1.24 s for a PDMS droplet inside PIB (T = 50 °C), $\eta_1 = 36$ Pa.s, $\eta_2 = 5$ Pa.s, $R_1 = 97$ μm, $R_2 = 77$ μm

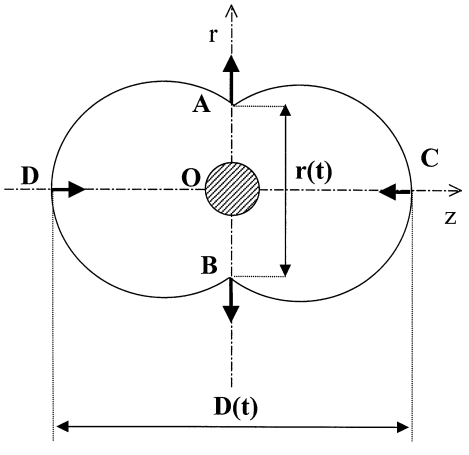

Fig. 7. Characteristic picture of the composite droplet. D(t) and r(t) are also shown, as well as elongational flow region location (*shaded circle*) and typical velocity vectors

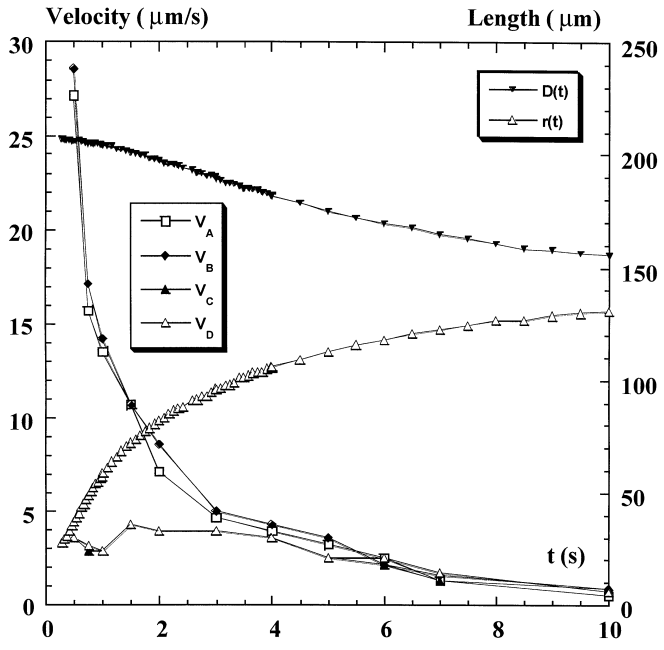

Fig. 8. PDMS droplets in PIB (T = 50 °C). Characteristic velocities at points A, B, C, D. D(t) and r(t) also plotted vs time t (data from Fig. 5)

when possible, and in some cases extrapolation techniques were used, because it is not always possible to have a particle velocity at the exact position. Nevertheless, this technique provides reasonable data, consistent with the photographs.

The velocity of points A and B ("neck ring") decreases until it reaches zero. Still it should be pointed out that the velocity at such points is zero at the start, and increases very rapidly and should probably go through a maximum. Due to the uncertainly of measurements at small times, only confident data points are shown (above 0.5 s). At very short times (scaling as $R^{3/2}$) smaller than 1 s, one may refer to the work of Eggers et al. (1999) for a scaling analysis.

At points C and D the velocity is most probably increasing first (before 1 s) then shows a plateau (from 1 s to 4 s) during the coalescence (or fusion) process, then finally drops out until it reaches zero. The final decrease is associated to relaxation of the droplet.

The distance r(t) has been used on several occasions and is also of great interest, as shown for example in the sintering problem, both theoretically and experimentally. Kuczynski (1949) studied self-diffusion of metallic particles, and Frenkel (1945) investigated the case of crystalline bodies, finding the distance to vary like $t^{0.5}$ which is in agreement with experiments. On the other hand, when viscoelastic effects prevail (Mazur and Plazek 1994), and if $r(t) \approx t^n$, then n can vary between 0.2 and 0.9, and is related to the viscoelastic behavior through the compliance. Finally Eggers (1998) found a theoretical exponent of 1/7 and a numerical one of 1/6, but in the case of surface diffusion. In our experiment, we determine the distance r(t) which is plotted in Fig. 9 in log-log scale, in order to measure the exponent n.

We have limited ourselves to data for which r(t) is measurable, i.e., times larger that about 0.24 s. In addition, there is light diffusion at the interface, which is also observed for example in Fig. 5a, and this renders the measurements difficult. We find a power dependence (Fig. 9) of the type

$$r(t) \approx t^{2/3} \tag{4}$$

This dependence is valid at small times and is in reasonable agreement with previous observations mentioned above, such as the ones corresponding to Newtonian fluids. Eggers and coworkers (Eggers et al. 1999) propose to scale r(t) as A t $\ln(t/t_0)$, where A and t_0 are fluid dependent constants. Unfortunately, this does not correspond to our data. At larger times the dependence is no longer valid but it is to be remembered that the theory (Frenkel 1945) is only valid for short times, due to the assumptions on the initial droplet shapes. Also this exponent may depend on p, which was not discussed in previous works.

Finally, data showing the velocity of points along the z-axis is shown in Fig. 10. This is done at different times of 0.24 s, 1 s, 3 s, and 8 s. This data is relevant for discussing elongational flows.

The symmetry of the droplet with respect to the (Orθ) plane (where θ is the usual polar angle) is emphasized again through the velocity profile symmetry. In addition, the central region of flow gives evidence of a linear dependence of the velocity vs distance z, as shown by the straight lines going through the data points. This is typical of an elongational flow, which has a velocity component proportional to the distance. In this graph, the width L_t of the linear region is also presented, which

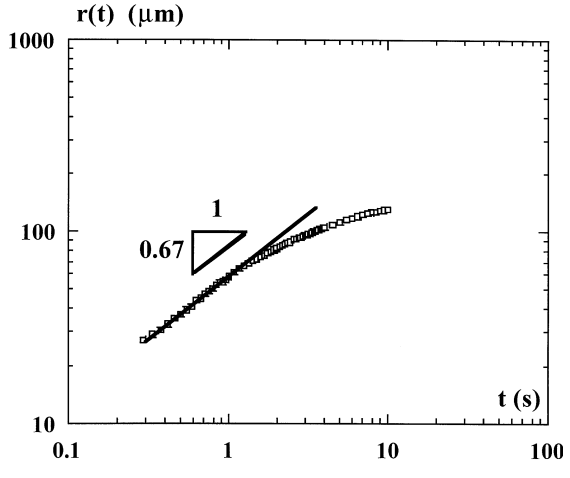

Fig. 9. Distance r(t) as a function of time t (data from Fig. 5)

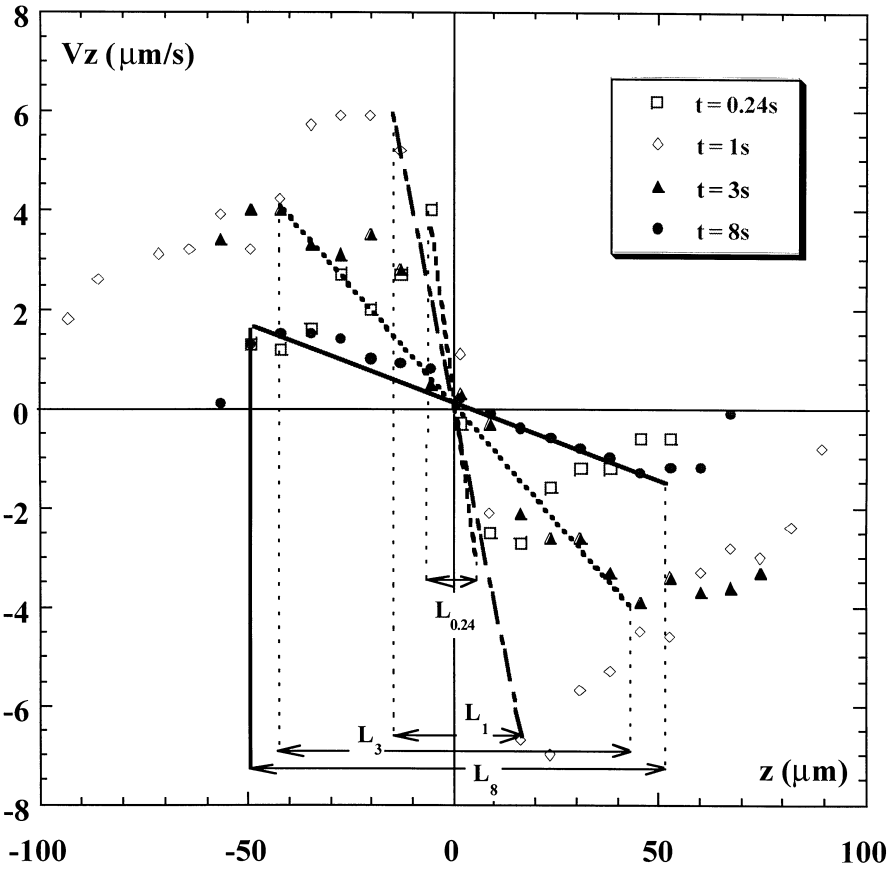

Fig. 10. Velocity V_z of the points along the z-axis. *Straight lines* are drawn to fit the data close to the center, corresponding to the elongational region of length L_t (data at times t = 0.24 s, 1 s, 3 s, 8 s)

shows the size of the elongational region of flow. This will be discussed in the next part.

Discussion

The coalescence experiment discussed in this work has two interesting features associated with it. It is first shown to be a nice way to have access to a relationship between the coalescence time and the viscosity ratio through a simple relation. Therefore it can be used conversely to estimate the interfacial tension once the viscosities of the fluids are known. The only data needed is the time dependence of the resulting droplet length, from which the so-called coalescence time is determined. Previous methods for determining the interfacial tension between polymer melts can then be compared.

The spinning drop tensiometry (Vonnegut 1942), its application to polymers (Elmendorp and de Vos 1986; Joseph et al. 1992), the pendant drop method (see for example Kamal et al. 1997), the filament thread method (Cohen and Carriere 1989), the embedded disk retraction method (Rundqvist et al. 1996), the ellipsoidal drop retraction (Luciani et al. 1997) or combinations of such methods (filament thread method – ellipsoidal retraction, Tjahjadi et al. 1994), all require a very well designed drop or filament to be inserted into another polymer, which is sometimes very difficult. In our instrument, all that is needed is to mix two polymers without having to worry about shaping droplets. The drainage part (Chesters 1991) is of course the longest part, but since many droplets can be chosen, this problem is properly handled. Finally, the coalescence process may require a long time, but it is to be remembered that only the first (short) part is of interest until the inflexion point on the D(t)-curve is found. Note also that some methods (i.e., spinning droplet, pendant drop) also require very long times when used with highly viscous polymers. Therefore this technique, coupled with a high temperature control now available with most microscopes, may be promising for measuring the interfacial tension after an exact solution is found corresponding to Eq. (3).

It may also provide valuable information such as the diffusion of copolymers when inserted at the interface or elsewhere in the fluid. Indeed, the time dependence of the drop size change has been shown to be a valuable tool for measuring diffusion coefficients of copolymers using a spinning drop tensiometer (Gaines and Bender 1972; Verdier et al. 2000).

The second important part of the experiment has been devoted to understanding flow fields using Particle Image Velocimetry (PIV). The methodology is shown to be well adapted for measuring flow fields in small-scale systems, as long as the particles are small enough (order of a micron or smaller if possible). Using droplets of diameters about 100 μm seems to be a good compromise. The velocity field is time dependent and reveals the presence of an elongational region in the center of the droplets (region defined in Fig. 7). Due to the linear relationship obtained between v_z and z (Fig. 10) at a given time, we postulate a flow field of the following type in the central region, when droplets are of equal size:

$$v_r = \dot{\varepsilon} r \quad v_\theta = 0 \quad v_z = -2\dot{\varepsilon} z \tag{5}$$

where $\dot{\varepsilon}$ is the elongational rate, a function of time, in the uniaxial elongational region and has been chosen so that it is always positive in our case. $\dot{\varepsilon}$ may be deduced from Fig. 10 using Eq. (5). The fact that the azimuthal componen v_θ is zero is related to our observations but also seems to make sense. All the movies made have demonstrated that no apparent distortion or droplet shear with respect to the other axes exist: the only shear is in the (Orz) plane. At least this is what is observed during the experiment time, and is certainly true close to the central region. The component along the z-axis is chosen to be proportional to z, as shown in Fig. 10, and the r-component of the velocity is simply chosen to satisfy a uniaxial elongational flow, as well as mass conservation.

The size of the elongational flow region is time dependent, as shown in Fig. 5a–f. By simple inspection of the flow field, it can be deduced that the region of elongation is very small at the beginning and that it is larger and larger as time goes on. Indeed, Fig. 5d–f shows that the elongational flow region has almost completely invaded the droplet volume. This is again verified in Fig. 10, where the size L_t of the region of elongation at time t (v_z is a linear function of z) is shown for t = 0.24 s, t = 1 s, t = 3 s, t = 8 s. This size is increasing with time. Qualitatively, this region is close to a spherical domain (from Fig. 5a–f). Finding an elongational region has been also discussed previously (Rallison 1980). Note that for different droplet sizes, this flow field does not obey the same formula at Eq. (5), but may probably be deduced by rescaling r and z. Figure 6 shows that the elongational region still exists, but is no longer symmetric.

The dependence of the flow field on time (for equal droplets) can be postulated to be of the type $\dot{\varepsilon} = \dot{\varepsilon}(t)$, still in the neighborhood of point O (Fig. 7). It is hard to give a simple form of $\dot{\varepsilon}(t)$, as only few experiments can be detailed here, but it is reasonable to think that the magnitude of the flow is related to $\dot{\varepsilon}(t)$, and that $\dot{\varepsilon}(t)$ is a rapid increasing function of time then a decreasing one (Fig. 11), after reaching a maximum in between. This is also checked by looking at velocity of point A. Figure 11 shows the expected variation of $\dot{\varepsilon}(t)$, with a few data points taken from the linear slope of v_z in Fig. 10.

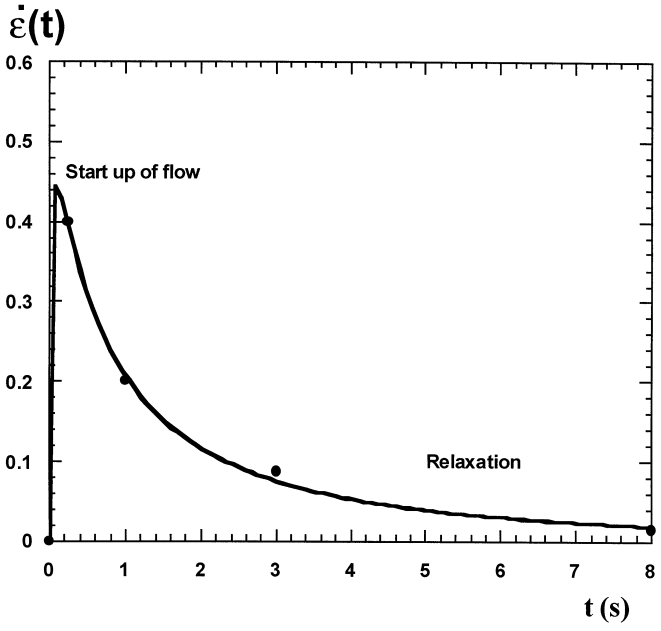

Fig. 11. Typical dependence of $\dot{\varepsilon}(t)$ as a function of time (points calculated from Fig. 10). The *line* is only a guide for the eye

Finally, the measurement of $\dot{\varepsilon}(t)$ may be very useful to have access to other rheological properties. In particular, at larger times, Fig. 11 may be used to determine the time-dependent properties of a two-fluid system, but this requires more attention and is not the purpose of the present study. Such analyses have been attempted before (Joseph et al. 1992) and reveal the complexity of such two-phase systems. The interface viscoelasticity may also be investigated. However, the main idea would be to consider other viscoelastic systems for such purposes.

Finally, an accurate determination of the flow field should allow to calculate the dissipations at the neck, and this may be useful to model the dependence of the coalescence time as a function of the viscosity ratio theoretically.

Conclusions

In this study it has been demonstrated that the coalescence experiment can be a very useful tool for estimating the interfacial tension of a polymer-polymer system. The effect of the viscosity ratio and droplet sizes has been understood. In addition, the system has been investigated further to evaluate velocity fields. It is clearly shown that

the flow field within droplets is a time-dependent one, close to a uniaxial extension inside the droplets.

These results, combined with an exact theory, may be used further to determine the interfacial tension of more complex systems (with copolymers, different architectures, chain lengths, etc.). Results giving the flow field may also be useful for comparison with numerical simulations involving droplet deformations.

Acknowledgements The authors are very thankful to Hélène Galliard, for helpful contribution to the PIV experiments.

References

Barthès-Biesel D, Acrivos A (1973) Deformation and burst of a liquid droplet freely suspended in a linear shear field. J Fluid Mech 61:1–21

Bentley BJ, Leal LG (1986) An experimental investigation of drop deformation and breakup in steady, two-dimensional linear flows. J Fluid Mech 167:241–283

Brochard-Wyart F, de Gennes PG (1992) Dynamics of partial wetting. Adv Colloid Interface Sci 39:1–11

Brochard-Wyart F, de Gennes PG (2000) Unpublished result

Chesters AK (1991) The modeling of coalescence processes in fluid-liquid dispersions: a review of current understanding. Trans Inst Chem Eng 69(A):259–270

Cohen A, Carriere CJ (1989) Analysis of a retraction mechanism for imbedded polymeric fibers. Rheol Acta 28:223–232

Eggers J (1998) Coalescence of spheres by surface diffusion. Phys Rev Lett 80(12):2634–2637

Eggers J, Lister JR, Stone HA (1999) Coalescence of liquid drops. J Fluid Mech 401:293–310

Elmendorp JJ, de Vos G (1986) Measurement of interfacial tensions of molten polymer systems by means of the spinning drop method. Polym Eng Sci 26(6):415–417

Fortelny I, Zivny A (1995a) Theory of competition between breakup and coalescence of droplets in flowing polymer blends. Polym Eng Sci 35(23):1872–1877

Fortelny I, Zivny A (1995b) Coalescence in molten quiescent polymer blends. Polymer 36(21):4113–4118

Frenkel J (1945) Viscous flow of crystalline bodies under the action of surface tension. J Phys USSR 9(5):385–391

Gaines GL, Bender GW (1972) Surface concentration of a styrene-dimethylsiloxane block copolymer in mixtures with polystyrene. Macromolecules 5(1):82–86

Grace HP (1982) Dispersion phenomena in high viscosity immiscible fluid systems and application of static mixers as dispersion devices in such systems. Chem Eng Commun 14:225–277

Grizzuti N, Bifulco O (1997) Effects of coalescence and breakup on the steady-state morphology of an immiscible polymer blend in shear flow. Rheol Acta 36:406–415

Guido S, Greco F (2001) Drop shape under slow steady shear flow and during relaxation. Experimental results and comparison with theory. Rheol Acta 40:176–184

Janssen JMH, Meijer HEH (1995) Dynamics of liquid-liquid mixing: A 2-zone model. Polym Eng Sci 35(22):1766–1780

Joseph DD, Arney MS, Gillberg G, Hu H, Hultman D, Verdier C, Vinagre TM (1992) A spinning drop tensioextensiometer. J Rheol 36(4):621–662

Kamal MR, Demarquette N, Lai-Fook RA, Price TA (1997) Evaluation of thermodynamic theories to predict interfacial tension between polystyrene and polypropylene melts. Polym Eng Sci 37(5):813–825

Kuczynski GC (1949) Self-diffusion in sintering of metallic particles. Trans Am Inst Mech Eng 185:169–178

Longin P-Y (1999) PhD Thesis, Université Grenoble I. Caractérisation ultrasonore de polymères et d'alliages de polymères

Luciani A, Champagne MF, Utracki LA (1997) Interfacial tension coefficient from the retraction of ellipsoidal drops. J Polym Sci B Polym Phys 35:1393–1403

Martula DS, Hasegawa T, Lloyd DR, Bonnecaze RT (2000) Coalescence-induced coalescence of inviscid droplets in a viscous fluid. J Colloid Interface Sci 232:241–253

Mazur S, Plazek DJ (1994) Viscoelastic effects in the coalescence of polymer particles. Prog Org Coat 24:225–236

Rallison JM (1980) Note on the time-dependent deformation of a viscous drop which is almost spherical. J Fluid Mech 98:625–633

Rallison JM (1984) The deformation of small viscous drops and bubbles in shear flows. Annu Rev Fluid Mech 16:45–66

Rundqvist T, Cohen A, Klason C (1996) The imbedded disk retraction method for measurement of interfacial tension between polymer melts. Rheol Acta 35:458–469

Stone HA (1994) Dynamics of drop deformation and breakup in viscous fluids. Annu Rev Fluid Mech 26:65–102

Stone HA, Leal LG (1989) The influence of initial deformation on drop breakup in subcritical time-dependent flows at low Reynolds numbers. J Fluid Mech 206:223–263

Sundararaj U, Macosko CW (1995) Drop breakup and coalescence in polymer blends: the effects of concentration and compatibilization. Macromolecules 28(8):2647–2657

Taylor GI (1934) The formation of emulsions in definable fields of flow. Proc R Soc 29:501–523

Tjahjadi M, Ottino JM, Stone HA (1994) Estimating interfacial tension via relaxation of drop shapes and filament breakup. AIChE J 40(3):385–394

Verdier C (2000) Coalescence of polymer droplets: experiments on collision. C R Acad Sci IV 1:119–126

Verdier C (2001) The influence of the viscosity ratio on polymer droplet collision in quiescent blends. Polymer 42:6999–7007

Verdier C, Vinagre HT, Piau M, Joseph DD (2000) High temperature interfacial measurements of PA6/PP interfaces compatibilized with copolymers using a spinning drop tensiometer. Polymer 41:6683–6689

Vinckier I, Moldenaers P, Terracciano AM, Grizzuti N (1998) Droplet size evolution during coalescence in semi-concentrated model blends. AIChE J 44(4):951–958

Vonnegut B (1942) Rotating bubble method for the determination of surface and interfacial tension. Rev Sci Instrum 13:6–9

Wagner M, Wolf BA (1993) Interfacial tension between poly(isobutylene) and poly(dimethylsiloxane): influence of chain length, temperature, and solvents. Macromolecules 26(24):6498–6502

Wu S (1982) Polymer interface and adhesion. Marcel Dekker, New York